Improving Inelastic Confinement-Induced Resonances calculations on the CRC model

T. Sanchez-Pastor,[1] Alejandro Saenz,[2] and F. Revuelta[1]

[1] *Grupo de Sistemas Complejos, Escuela Técnica Superior de Ingeniería Agronómica, Alimentaria y de Biosistemas, Universidad Politécnica de Madrid, Avda. Puerta de Hierro 2-4, 28040 Madrid, Spain.*

[2] *AG Moderne Optik, Institut für Physik, Humboldt-Universität zu Berlin, Newtonstrasse 15, 12489 Berlin, Germany.*

In this work we study several aspects of the Inelastic Confinement-Induced Resonances caused by the coupling of center-of-mass and relative motion for a system of two Lithium ultracold atoms in anharmonic sextic traps. We take advantage of the *ab initio* calculations to ensure the CRC model robustness presented in [Phys. Rev. Lett. **109** 073201 (2012)] computing the exact trap relative motion energy of the resonance. We generalize the theoretical resonance position as a function of a parameter $\mathcal{C}$ and give exact results of the theory predictions for a wide range of this parameter in 3-D and quasi 1-D optical traps. Shadow bands corresponding to the predictive limit of the theory are also presented. Within the theoretical results we also study the main differences between both confinements. Finally, we build a perturbative model in order to describe in depth the origin of the asymmetric splitting of the resonances.

I. INTRODUCTION

Contar un poco de historia de la observación de este tipo de resonancias, por qué los sistemas ultrafríos están de moda (control) y resonancias de Feshbach (cambiar B es cambiar a). Acoplamiento CM-rm como causante de los cruces evitados, transiciones no adiabáticas y rmacionarlo con el teorema adiabático.

II. TWO-ATOM NUMERICAL SIMULATIONS

In this section we present the Hamiltonian that describes the interaction between two ultracold-atoms trapped in anisotropic optical lattices (Sec.II A). Also, ab initio calculations to simulate the system is presented in Sec.II B.

A. Hamiltonian

The system is formed by two Lithium ultracold atoms that interact only via s-wave scattering due to the extremely low temperature of the gas. The last leads to a spatial symmetry where rm andCM coordinates reduce the complexity of the calculations. Relative motion distance is defined as $\boldsymbol{r} = \boldsymbol{r_1} - \boldsymbol{r_2}$ whereas CM coordinate as $\boldsymbol{R} = \frac{1}{2}(\boldsymbol{R_1} + \boldsymbol{R_2})$. The Hamiltonian is then given by:

$$\begin{aligned}\mathcal{H}(\boldsymbol{r},\boldsymbol{R}) = T_{CM}(\boldsymbol{R}) + T_{rm}(\boldsymbol{r}) + V_{CM}(\boldsymbol{R}) + \\ + V_{rm}(\boldsymbol{r}) + W(\boldsymbol{r},\boldsymbol{R}) + U_{int}(|\boldsymbol{r}|),\end{aligned} \tag{1}$$

where the T's are the kinetic energy operators and the V's the separable potential energies for both rm and CM coordinates, while W accounts for the rm-CM coupling, which is nonzero for anharmonic traps. The coupling term is responsible of the avoided crossings and therefore of the ICIR. U_{int} is the particle-particle potential energy often described in analytic derivations by the pseudopotential $U_{int} = \frac{4\pi\hbar^2 a_s}{m}\delta(\boldsymbol{r})\frac{\partial}{\partial \boldsymbol{r}}$, where a_s is the 3-D s-wave scattering length.

In a 3-dimensional optical trap the potential terms are

$$V_{rm}(\boldsymbol{r}) = 2\sum_{j=x,y,z} V_j \sin^2\left(\frac{1}{2}kr_j\right), \tag{2}$$

$$V_{CM}(\boldsymbol{R}) = 2\sum_{j=x,y,z} V_j \sin^2\left(kR_j\right), \tag{3}$$

$$W(\boldsymbol{r},\boldsymbol{R}) = -4\sum_{j=x,y,z} V_j \sin^2\left(\frac{1}{2}kr_j\right)\sin^2\left(kR_j\right). \tag{4}$$

k is the angular wavenumber and V_j the potential depth in any direction. Associated with the potential depth, the trap frequencies are $\omega_j = k\sqrt{\frac{2V_j}{m}}$ and the characteristic trap length $d_j = \sqrt{\frac{2\hbar}{m\omega_j}}$. Thus, the anisotropies can be defined in units of the transversal component: $\eta_j = \frac{\omega_j}{\omega_y}$.

B. Ab Initio calculations

Schrödinger equation is solved using the full six-dimensional Hamiltonian of eq.(1) in spherical coordinates. The exact diagonalization is carried using realistic short-range interatomic potentials: numerically Born-Oppenheimer curves. The interaction potential is then varied to tune the scattering length. Regarding the trap potential we expand to sixth order to account for anisotropies associated with non-vanishing coupling terms. We use a basis set of B-splines and spherical harmonics for the angular dependencies. [1]

The computation of the eigenenergies and eigenfunctions is obtained in a two-step method as follows: (i) First, the separable part of the Hamiltonian is diagonalized in order to compute the eingenfunctions $|\psi_n^{rm}\rangle$ and $|\Psi_{\boldsymbol{m}}^{CM}\rangle$, which will be called *orbitals* because of their sim-

ilarity to the electronic orbitals used in Quantum Chemistry. (ii) The coupling remaining term is solved building a new basis. The states of this basis are the so-called *configurations* $|\Phi_{n,\boldsymbol{m}}\rangle = |\psi_n^{rm}\Psi_{\boldsymbol{m}}^{CM}\rangle$.

Ab initio calculations are used to compute the dependence of the eigenenergies on the scattering length for a wide range of anisotropies η_x. The center points of the avoided crossings are the positions of the ICIR that we compare with the theory predictions.

III. IMPROVING ICIR CALCULATIONS

This section is devoted to dig into the CRC model used in other works to predict the ICIR positions. First, we explain its main assumptions, limitations of the model and we propose a method to compare ab initio and model predictions. In Sec. III A we present the results for a 3-D trap: the complete dependence of the spectrum on the scattering length a_s and the resonance positions for numerous anisotropies. Finally, we present similar results for a quasi 1-D trap in Sec. III B.

In order to locate the resonance in the energy spectrum, exact solutions of the anharmonic traps are needed. However, an exact solution remains unknown yet. In contrast to this, an exact solution has recently been developed for fully anisotropic harmonic confinements in [2] and in [3], where the solutions of [4] and [5] have been generalized.

ICIR have its origin in the avoided crossings between the relative least bound state with CM excitations $|\psi^{(b)}(\boldsymbol{r})\Psi_{\boldsymbol{n}}(\boldsymbol{R})\rangle$ and the lowest trap state $|\psi^{(1)}(\boldsymbol{r})\Psi_{(0,0,0)}(\boldsymbol{R})\rangle$ (next excited states of the trap are empty due to low thermal energies). Thus, the crossings satisfy the relation: $E_b = E_1$, where the bound state energy is $E_b = E_b^{rm} + E_{\boldsymbol{n}}^{CM}$ and the trap state energy $E_1 = E_1^{rm} + E_{(0,0,0)}^{CM}$. Theory provides an analytic expression to implicitly relate the bound relative energy with the scattering length as follows:

$$\frac{\sqrt{\pi}d_y}{a_s} = -\int_0^\infty dt\left(\frac{\sqrt{\eta_x\eta_z}e^{\frac{\epsilon t}{2}}}{\sqrt{(1-e^{-t})(1-e^{-\eta_x t})(1-e^{-\eta_z t})}} - t^{-\frac{3}{2}}\right). \tag{5}$$

$\epsilon = \frac{E_b^{rm}-E_0}{\hbar\omega_y}$ is the energy shift and $E_0 = \frac{\hbar}{2}\sum_j \omega_j$ the ground state energy of the CM for a harmonic trap. Using the above expressions the energy shift can be described by:

$$\epsilon = \frac{E_1^{rm} - E_{\boldsymbol{n}}^{CM} + E_0^{CM} - E_0}{\hbar\omega_y} \tag{6}$$

The two cornerstones of the CRC model are: (i) assume the anharmonicities are small enough to be treated as perturbations. (ii) The ICIR occurs when the eigenenergy E_1^{rm} of the first trap state $|\psi^{(1)}\rangle$, which lies in the interval $[E_0, E_0 + 2\hbar\omega_z)$, is $E_1^{rm} = E_0 + \hbar\omega_z$ [6]. In this work, we study the validity of the second assumption considering the ICIR to happen at

$$E_1^{rm} = E_0 + \mathcal{C}\hbar\omega_z, \tag{7}$$

where $\mathcal{C} \in [0, 2)$ is a parameter to determine using the ab initio ICIR positions. As will be later demonstrated, in the case of quasi 1-D traps, the assumption of $\mathcal{C} = 1$ works relatively fine, but when more CM excitations are present or the trap is not excessively anisotropic, a smaller value of $\mathcal{C}$ is more accurate. Therefore, subsituying Eq. 7 into Eq. 6

$$\epsilon = C\eta_z - \frac{E_{\boldsymbol{n}}^{CM} - 2E_0^{CM} + E_0}{\hbar\omega_y} \tag{8}$$

Recall that $\mathcal{C}\hbar\omega_z$ gives the energy difference between the resonance energy and the asymptotic energy E_∞ of the first excited state for $\frac{d_y}{a_s} \to \infty$ (limit of noninteracting particles). Then, the $\mathcal{C}$ parameter can be computed as

$$\mathcal{C} = \frac{E_{ICIR} - E_\infty}{\hbar\omega_z}. \tag{9}$$

In this manner, this approach accounts for trap anharmonicities since E_∞ is chosen the energy of the asymptotic configuration. Furthermore, the energy of the resonance E_{ICIR} is obtained with ab initio calculations, which means that also takes into account the coupling terms.

A. 3-D

We start the calculations in the totally symmetric trap, where the eigenenergies are degenerated in the three spatial directions. As said, the scattering length is tuned while changing the Born-Oppenheimer potential. Thus, the fully coupled-adiabatic spectrum is shown in Fig.2.a). The CM excited bound states can be easily identified due to they tend to zero when the scattering length also tends to zero. The lowest curve corresponds with the ground state $|\psi^{(b)}\Phi_{(0,0,0)}\rangle$ and the next three degenerated states with two CM excited bound states. Close to them we found the first trap state $|\psi^{(1)}\Phi_{(0,0,0)}\rangle$ that only causes resonances for repulsive potentials ($a_s > 0$).

The width of the avoided crossings is proportional to the coupling strength, therefore the existence of resonances is governed by the laser intensities. A key feature of the 3-D case is that all spatial directions can contain resonances. Unfortunately, the resonances of $|\psi^{(b)}\Phi_{(2,0,0)}\rangle$ and $|\psi^{(b)}\Phi_{(0,2,0)}\rangle$ are not found to every value of the anisotropy η_x as for the quasi 1-D case, despite of that we study the resonances $|\psi^{(b)}\Phi_{(4,0,0)}\rangle$ and $|\psi^{(b)}\Phi_{(0,4,0)}\rangle$.

In Fig. 1. b) the adiabatic and diabatic energies are represented, as well as de ICIR positions. The effect of

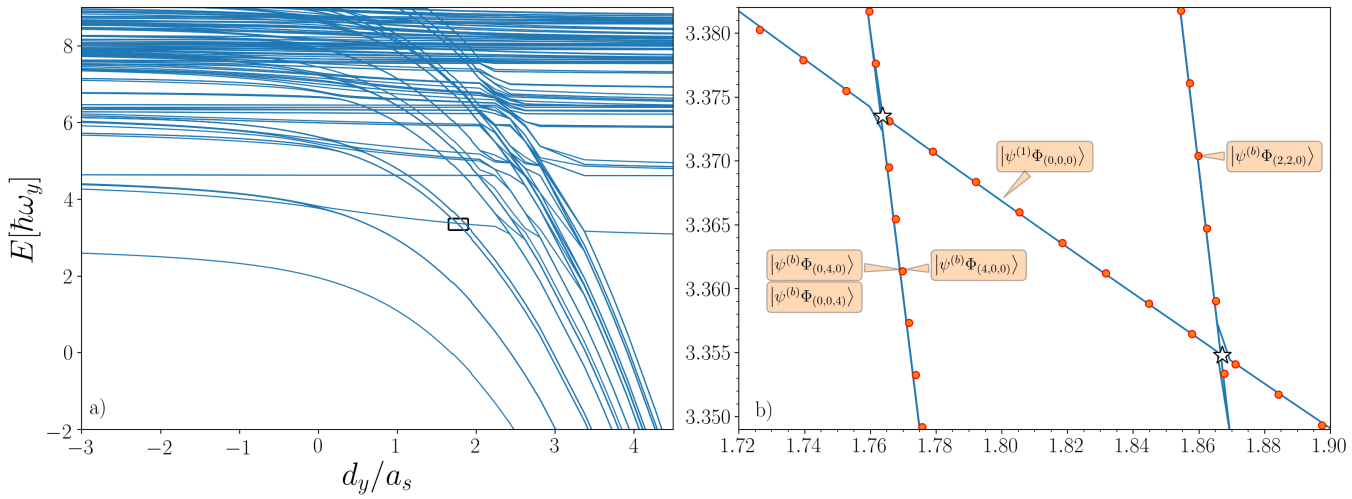

Figure 1: a) Adiabatic Spectrum of the full coupled Hamiltonian for ^{7}Li atoms confined in an isotropic sextic trapping potential with $V_x = V_y = V_z = 35.9E_R$, $\eta_x = \eta_y = 1$ and $\lambda = 1000$ nm where $E_R = \frac{\hbar^2 k^2}{2m}$ is the photon recoil energy. All states bending down to $-\infty$ are molecular states originating from the rm bound state $\psi^{(b)}$ with different CM excitations, whereas the states remaining constant are trap states of different rm excitations $\psi^{(1)}$ and zero CM excitations. Black square zoom in figure b) where diabatic levels are plotted with orange circles and labeled by kets. White stars represent the cross between trap and bound CM excited states, i.e. the ICIR.

increasing the longitudinal anisotropy on the spectrum resides in a breaking of symmetry of the trap. The energy degeneracy is also broken and the isotropic resonance splits in two.

Repeating the same calculations for longitudinal anisotropies η_x from 1 to 1.25 leads to a wide range of ICIR positions. These positions will be further used to computing the $\mathcal{C}$ parameter with the Eq.(7) and thus validate the CRC model. Each resonance has four predictions associated with it depending on the value of the parameter: exact $\mathcal{C}$ arising from the exact ICIR position, $\mathcal{C} = 1$ corresponding to the assumption of previous works, the lower limit $\mathcal{C} = 0$ and the upper limit $\mathcal{C} = 2$. Limit values serve to constrain the predictions of the theory, they will be represented by shadow bands where each of the four previous predictions will fall within them. With regard to the excitation energies of the CM, they have been calculated numerically using a sinc-DVR method.

Figure 2 contains the ICIR's position as a function of the longitudinal anisotropy η_x of the *ab initio* calculations and the modified CRC model. The mean value and the deviation of the set of exact $\mathcal{C}$ obtained for all the resonances are $\mathcal{C} = 0.52 \pm 0.03$. In addition, the mean absolute error (MAE) between the prediction and the *ab initio* calculations is $1.6 \cdot 10^{-2}$. On the other hand, the MAE obtained using $\mathcal{C} = 1$ is $7.3 \cdot 10^{-2}$, four times greater than for the exact $\mathcal{C}$. The origin of this discrepancy between the second CRC model assumption and our calculations is more pronounced in the 3-D case, as a result of the extreme level mixing characteristic to this confinement dimension that displaces the diabatic crossings from the isotropic harmonic case. We will further

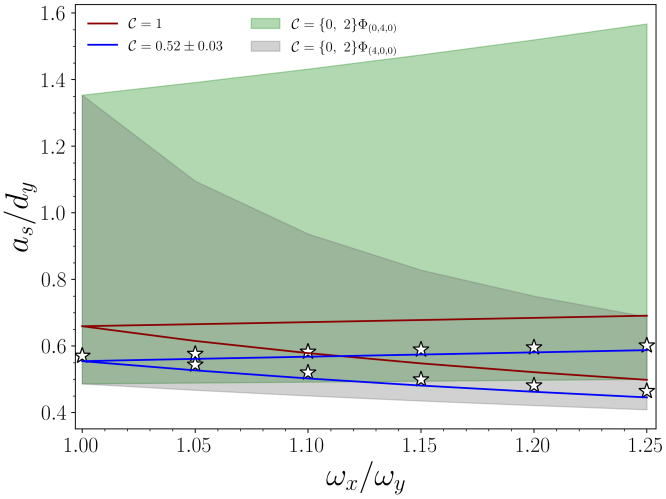

Figure 2: Positions of the ICIR associated with four CM excitations in terms of the characteristic transversal length for different values of transversal anisotropy in 3-D. White stars become from ab initio calculations, blue solid lines the exact theory computations, red solid lines $\mathcal{C} = 1$, gray shadows the corresponding theory computations with both $C = 2$ and $C = 0$ for the longitudinal resonances and green shadows for the transversal resonances.

discuss this result in Sec. III B. Concerning the shadow bands, it is interesting the fact that $\mathcal{C} = 0$ achieve better results than $\mathcal{C} = 2$ for every anisotropy and it is ununderstandable without a proper perturbative approach.

In the same line, asymmetric splittings of the ICIR between the limit values are explained within perturbative schemes in Sec. IV.

We have verified that using *ab initio* calculations to compute the ICIR position is necessary in 3D confinements; on the one hand the exact $\mathcal{C}$ yields better results than the prior assumption, on the other hand the predictions dispersion (delimited by the shadow bands) is quite large. This analysis found evidence of the effect of the extreme level mixing that motivates to expand the study to a case of negligible mixing, the quasi 1-D confinement.

B. quasi 1-D

Quasi 1-D confinement states for an extreme anisotropy in a given direction of space where the level interaction with the other two directions can be neglected i.e. $\omega_z \ll \omega_x, \omega_y$. Thus, the trap length is $d_z \gg d_x, d_y$ leading to a confinement that has a form of a 1-D tube with the Z-axis being the longitudinal direction whereas X and Y axis are the transversal directions. This regime can be described by the quasi 1-D approximation in Eq. (5), which provides good results for anisotropies of $\eta_z = 0.1$. However, in what follows we keep using the complete equation to avoid small variations and make the computations as exact as possible.

The spectrum follows the same pattern than the 3-D case: excited CM states and trap states. Instead, now the resonances of $|\psi^{(b)}\Phi_{(2,0,0)}\rangle$ and $|\psi^{(b)}\Phi_{(0,2,0)}\rangle$ are found and they are the ones chosen to test the modified CRC model, in the same line that the previous study. The degeneracy exists when the longitudinal directions are isotropic, nevertheless, increasing the longitudinal anisotropy eta_x erases the degeneracy, leading to a similar splitting of the resonances than in 3-D.

Same calculations are performed to obtain the results shown in Fig. 3. The results are substantially better than in 3-D, the exact $\mathcal{C}$ is 0.81 ± 0.01 demonstrating that the assumption of the CRC model was not exactly accurate. Still, the predictions of $\mathcal{C} = 1$ satisfactory reproduce the resonances positions. From this results is clear that the quasi 1-D case is more insensitive to the change of $\mathcal{C}$, this can be easily understand by looking at Eq. (8) where the dependence on $\mathcal{C}$ is modulated by the anisotropy in the z direction. In the quasi 1-D trap $\eta_z = 0.1$ while in the 3-D trap $\eta_z = 1$. Regarding the MAE obtained we found that $\mathcal{C} = 1$ and the exact one are statistically equal, for both predictions the MAE is $6.1 \cdot 10^{-3}$. Finally, the shadow bands are much more thicker than in 3-D.

Results demonstrate that the assumption of $\mathcal{C} = 1$ is not necessarily true for quasi 1-D and wrong for 3-D traps. The width of the shadow bands indicate that *ab initio* calculations are essential to compare theory with experiments, until exact solutions including the anharmonicities are found.

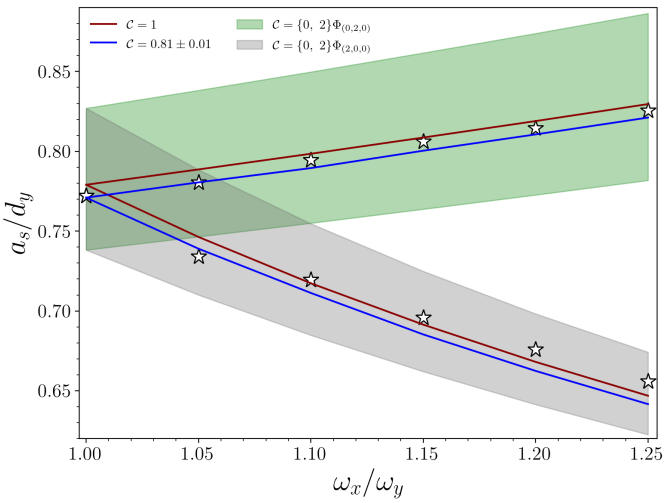

Figure 3: Same as Fig. 2 but in the quasi 1-D case with parameters: $V_y = 35.9E_R$, $\eta_z = 0.1$ and $\lambda = 1000$ nm.

IV. ORIGIN OF THE ASYMMETRIC SPLITTING OF THE ICIR

In this section we develop a perturbation theory to predict the position of an ICIR. As it will be shown, this perturbative scheme provides a simple explanation to the asymmetric splitting that is observed when the experimental setup becomes anisotropic by changing the longitudinal or the transversal frequencies.

In order to follow a self-consistent approach the perturbed CM energies are used. The anharmonic terms of the trapping potential are then treated as a perturbation. R^4 and R^6 terms are expressed in terms of the Hermite Polynomials to make the integrals exactly solvable, yielding to

$$\begin{aligned} E_{\boldsymbol{n}}^{CM} = & \sum_{j=x,y,z} \hbar\omega_j(n_j + 1/2) \\ & - \frac{1}{1152V_j^2}\left[36V_j\hbar^2\omega_j^2(2n_j^2 + 2n_j + 1)\right. \\ & \left. - \hbar^3\omega_j^3(4n_j^3 + 6n_j^2 + 8n_j + 3)\right] \end{aligned} \tag{10}$$

which is the first order perturbation term of the CM trapping potential, n_j are the excitation levels in a given direction. Equation (10) give the energy of a single well. The inclusion of higher order correction terms render a triple well, and, as a consequence, can be used to describe multiwell effects. Notice that the perturbative scheme is only meaningful up to $2l + 1$ order $\mathcal{O}(\hbar\omega_j)$, with $l = 0, 1, 2, ...$, as, otherwise, it yields unphysical results with negative energies, as they correspond to an unbounded potential associated with the Taylor expansion of the optical lattice. Consequently, the energy shift

is given by:

$$\epsilon = \mathcal{C}\eta_z - \sum_j \left[\eta_j n_j - \eta_j^2 \frac{\hbar\omega_y}{16V_j} n_j(n_j+1) - \eta_j^3 \left(\frac{\hbar\omega_y}{24V_j}\right)^2 n_j(4+3n_j+2n_j^2)\right]. \quad (11)$$

Thus, we take as reference the isotropic setting, which has a frequency $\bar{\Omega}$ in all directions, then a change in the frequencies can be written as

$$\omega_x = \bar{\Omega} + \Delta\omega_x, \quad (12)$$
$$\omega_y = \bar{\Omega} + \Delta\omega_y, \quad (13)$$
$$\omega_z = \bar{\Omega} + \Delta\omega_z. \quad (14)$$

Recall that any change in the frequencies will also affect the value of the characteristic length d_y, the η_x and η_z ratios, and the energy shift ϵ, which then will become

$$d_y = \bar{d_y} + \Delta d_y, \quad (15)$$
$$\eta_x = \bar{\eta_x} + \Delta\eta_x, \quad (16)$$
$$\eta_z = \bar{\eta_z} + \Delta\eta_z, \quad (17)$$
$$\epsilon = \bar{\epsilon} + \Delta\epsilon. \quad (18)$$

If we change the frequencies slightly all at once ($\Delta\omega_i \ll \omega_i$) the integral of Eq. (5) can be Taylor expanded. Although we are interested in the case of changing only ω_x.

The result of the expansion is presented in terms of integrals of the form

$$\mathcal{I}(\epsilon,\eta_x,\eta_z,d_y,A,B) = \frac{1}{\sqrt{\pi}d_y} \int_0^\infty dt \left(\frac{A\sqrt{\eta_x\eta_z}e^{\frac{\epsilon t}{2}}}{\sqrt{(1-e^{-t})(1-e^{-\eta_x t})(1-e^{-\eta_z t})}} - Bt^{-\frac{3}{2}}\right). \quad (19)$$

Note that the scattering length corresponds with $\frac{1}{a_s} = -\mathcal{I}(\epsilon,\eta_x,\eta_z,d_y,1,1)$. Then after the expansion we have

$$\frac{\bar{d_y}}{a_s} = -\mathcal{I}(\bar{\epsilon},1,1,1,1,1)\left(1-\frac{\Delta d_y}{\bar{d_y}}\right) - \mathcal{I}\left(\bar{\epsilon},1,1,1,\frac{t}{2},0\right)\Delta\epsilon - \mathcal{I}\left(\bar{\epsilon},1,1,1,\frac{1-e^{-t}(1+t)}{2(1-e^{-t})},0\right)\Delta\eta_x + \mathcal{O}(\Delta\eta_x)^2 + \mathcal{O}(\Delta\epsilon)^2. \quad (20)$$

We analyze up to first order in perturbation theory the imprint of a small change in the longitudinal frequency on the scattering length, and provide an explanation on the ICIR splitting, as schematically sketched in Fig. 4. We study the influence of a change in the longitudinal frequency, ω_x. The unique ICIR located at point A (cyan circle) for the isotropic setting will bifurcate into two different branches (cyan arrows). Notice that while the top branch increases abruptly, the bottom one is only slightly affected by the frequency change.

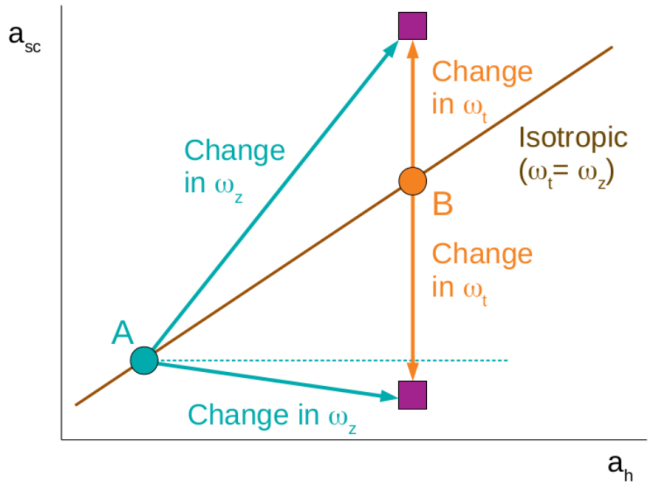

Figure 4: The inelastic confinement-induced resonances for the isotropic setting (brown line) bifurcate in two different branches when the traps becomes anisotropic. In point A (cyan circle), the longitudinal frequency (ω_x) is decreased,and then the two cyan branches separate rightwards, moving one of them upwards, while the other one remains almost constant. In point B (orange circle), the transversal frequencies ($\omega_y = \omega_z$) are increased, and then the two vertical orange branches separate one moving upwards and the other one downwards.

Changing only the longitudinal frequency implies $\delta d_y = 0$ since it remains constant. As in the experiment, we assume $\Delta\omega_x < 0$. Then

$$\Delta\eta_x = \frac{\Delta\omega_x}{\bar{\Omega}}, \quad (21)$$

which renders a negative contribution to the scattering length that tends to decrease ($a_s < \bar{a_s}$). Regarding the correction of the energy shift, the interpretation is more involved since it depends on the excitation level. The main contribution is

$$\Delta\epsilon \cong (n_x - \mathcal{C})\frac{|\Delta\omega_x|}{\bar{\Omega}}, \quad (22)$$

which is positive for $n_x > C$ and negative for $n_x = 0$.

Let us now discuss the different behavior of the ICIR's depending on whether they have excitations in the longitudinal direction, x, or not. On the one hand, when the ICIR has no CM excitations in the x direction, then the last two terms appearing in Eq. 20 will be negative, and, as a consequence, the value of the scattering length will be smaller than in the isotropic setting. Contrary, if the ICIR has some CM excitations in the x direction, the new scattering length will increase with the value of n_x, as the second term in Eq. 20 will be positive and dominates over the second one; Moreover, the increment

in the scattering length will increase with the number of excitations in the x direction, n_x, and, as a consequence, the ICIR splitting will become more asymmetric.

Finally, Eq. 22 can be used to explain the extreme asymmetry between the shadow bands in the 3-D case. In Fig. 2 the prediction obtained with the exact $\mathcal{C}$ is in better agreement to $\mathcal{C} = 0$ than 2. Substituting in the last expression for the energy shift $n_x = 4$ gives $\Delta\epsilon(\mathcal{C} = 0) = 4\frac{|\Delta\omega_x|}{\bar{\Omega}}$ and $\Delta\epsilon(\mathcal{C} = 2) = 2\frac{|\Delta\omega_x|}{\bar{\Omega}}$. The exact value of the parameter is 0.52 ± 0.03, which corresponds with $\Delta\epsilon(\mathcal{C} = 0.52) = 3.48\frac{|\Delta\omega_x|}{\bar{\Omega}}$. As presented in Eq. (5), the scattering length, a_s have an exponential dependence on the energy shift, as a consequence the asymmetry between both predictions is exponentially increased.

V. CONCLUSIONS

ANKNOWLEDGEMENTS

[1] Sergey Grishkevich, Simon Sala, and Alejandro Saenz. Theoretical description of two ultracold atoms in finite three-dimensional optical lattices using realistic interatomic interaction potentials. *Phys. Rev. A*, 84:062710, Dec 2011. doi:10.1103/PhysRevA.84.062710. URL `https://link.aps.org/doi/10.1103/PhysRevA.84.062710`.

[2] Yue Chen, Da-Wu Xiao, Ren Zhang, and Peng Zhang. Analytical solution for the spectrum of two ultracold atoms in a completely anisotropic confinement. *Phys. Rev. A*, 101:053624, May 2020. doi: 10.1103/PhysRevA.101.053624. URL `https://link.aps.org/doi/10.1103/PhysRevA.101.053624`.

[3] G. Bougas, S. I. Mistakidis, G. M. Alshalan, and P. Schmelcher. Stationary and dynamical properties of two harmonically trapped bosons in the crossover from two dimensions to one. *Phys. Rev. A*, 102:013314, Jul 2020. doi:10.1103/PhysRevA.102.013314. URL `https://link.aps.org/doi/10.1103/PhysRevA.102.013314`.

[4] Zbigniew Idziaszek and Tommaso Calarco. Analytical solutions for the dynamics of two trapped interacting ultracold atoms. *Phys. Rev. A*, 74:022712, Aug 2006. doi: 10.1103/PhysRevA.74.022712. URL `https://link.aps.org/doi/10.1103/PhysRevA.74.022712`.

[5] Jun-Jun Liang and Chao Zhang. Two ultracold atoms in a completely anisotropic trap. *Physica Scripta*, 77(2):025302, feb 2008. doi:10.1088/0031-8949/77/02/025302. URL `https://doi.org/10.1088/0031-8949/77/02/025302`.

[6] Simon Sala, Philipp-Immanuel Schneider, and Alejandro Saenz. Inelastic confinement-induced resonances in low-dimensional quantum systems. *Phys. Rev. Lett.*, 109:073201, Aug 2012. doi: 10.1103/PhysRevLett.109.073201. URL `https://link.aps.org/doi/10.1103/PhysRevLett.109.073201`.

[7] Thomas P. Fay, Lachlan P. Lindoy, David E. Manolopoulos, and P. J. Hore. How quantum is radical pair magnetoreception? *Faraday Discuss.*, 221:77–91, 2020. doi:10.1039/C9FD00049F. URL `http://dx.doi.org/10.1039/C9FD00049F`.